

Using Feature Detection and Richardson Extrapolation to Guide Adaptive Mesh Refinement for Vortex-Dominated Flows

Sean J. Kamkar, Antony Jameson, Andrew M. Wissink,
and Venkateswaran Sankaran

Abstract The article describes a Cartesian-based adaptive mesh refinement approach applied to vortex-dominated flows. Several distinct feature-detection methods are investigated to furnish a means for tagging cells for refinement. In each case, appropriate normalization is defined so that the process is automated for a range of operating conditions. Richardson extrapolation is proposed to assess the local error and terminate the mesh refinement once adequate error reduction is achieved.

1 Introduction

Many aerodynamics flowfields require the accurate resolution of vortices over long distances. Adaptive Mesh Refinement (AMR) provides an attractive means of achieving the desired accuracy in an efficient manner. Because the vortex transport occurs predominantly in the so-called “off-body” region of the flowfield, we adopt an overset-based dual-mesh paradigm [8] that utilizes unstructured grids in the near-body region and Cartesian meshes in the off-body region. The unstructured meshes provide ease of grid generation for complex geometries and accurately capture boundary layer effects. The Cartesian meshes allow the use of high-order discretization and ease of automation of the AMR process. The present article is focused on the development and implementation of algorithms for Cartesian-based AMR. The approach is based upon using feature-detection methods [6] for tagging off-body regions for refinement and Richardson extrapolation techniques [1, 7] for estimating the local error and terminating the refinement process. Specific attention is placed on automating the AMR process so that the methods can be applied to a variety of practical flowfields without need for user intervention.

S.J. Kamkar (✉)
Stanford University, Palo Alto, CA 94305, USA
e-mail: skamkar@stanford.edu

2 Feature Detection

Four feature detection methods are presented and tested in this work: (1) the Q -criterion [4], (2) the λ_2 criterion [5], (3) the eigenvalues of the velocity gradient tensor $\nabla \mathbf{u}$ [2], and (4) the correlation between the symmetric and antisymmetric parts of $\nabla \mathbf{u}$ [3]. All methods are presented in a non-dimensional form by imposing a local normalization, which emphasizes generality and automation. Specifically, the goal is to avoid any problem-dependent parameters that need to be tuned. For each method, a function, f_{val} is defined, which is used for purposes of vortex detection. A given cell is marked for refinement when the local value of the function exceeds a pre-specified threshold value, i.e., $f_{val} > t_{val}$.

Non-dimensional Q :

Using both the rotational (Ω) and strain (S) components of the velocity gradient tensor, i.e., $S = (\nabla \mathbf{u} + \nabla \mathbf{u}^T)/2$, $\Omega = (\nabla \mathbf{u} - \nabla \mathbf{u}^T)/2$, we can obtain a measure of the *relative* vortical strength [5]:

$$f_{val} = \frac{1}{2} \left(\frac{\|\Omega\|^2}{\|S\|^2} - 1 \right) \quad (1)$$

Non-dimensional λ_2 :

It can be shown that the tensor, $S^2 + \Omega^2$, approximately represents the pressure field in a flow. Therefore, the eigenvalues of this system can be used to determine pressure minima, which usually occur in or near vortex cores. If the eigenvalues are ordered in a fashion where $\lambda_1 \geq \lambda_2 \geq \lambda_3$, the condition $\lambda_2 < 0$ identifies the vortex core [6]:

$$f_{val} = -\frac{\lambda_2}{\|S\|^2} \quad (2)$$

Modified- Δ :

The eigenvalues of $\nabla \mathbf{u}$ reveal information about the local flow-field. For example, if a pair of complex eigenvalues is detected, swirling motion is present [2]. Furthermore, the magnitude of the complex conjugate (λ_{ci}) is a measure of the vortical strength:

$$f_{val} = \frac{\lambda_{ci}}{\|S\|} \quad (3)$$

S - Ω Correlation:

The three previous methods have been designed to pinpoint vortex cores; here, we examine a method that attempts to locate a vortex sheet. Specifically, we leverage the fact that strain and rotation rates are correlated, and that both have large magnitudes in vortex sheets [3]. λ_+ is the largest eigenvector orthogonal to the vorticity vector for the system $S\Omega - \Omega S$:

$$f_{val} = \frac{\lambda_+}{\|S\|^2} - 1. \quad (4)$$

In all the above methods, the functional value is used to mark mesh cells for refinement if its value is greater than the pre-specified threshold value, i.e., $f_{val} > t_{val}$. Each threshold function has a zero offset so that, in all cases, positive values represent regions of swirl. As an example, we consider the application of the modified- Δ method applied to the AMR-tracking of a propagating Lamb vortex. Figure 1 shows a snapshot of the solution at a particular time instance. The vortex is observed to be completely enclosed within the fine-grid region. Furthermore, as the solution advances through the domain, the fine grid properly tracks the feature and provides adequate resolution so that it is well resolved. At the end of the simulation, even after the vortex has travelled about 12 chord lengths, its initial coherent structure and strength remains relatively intact. Figure 1 also compares the non-dimensional Q , λ_2 , Δ , and $S-\Omega$ methods with the traditional vorticity-tagging method ($t_{val} = 8.67 \times 10^{-3}$). A solution computed on a uniformly fine mesh is also included. Additionally, the exact solution is provided for further validation. It is clear that the different feature detection techniques agree very closely with the exact solution as well as with the numerical predictions from the uniform fine mesh. It is important to note that, while the vorticity method also performs well, the vorticity magnitude has to be tuned for optimal performance for each case, while in the normalized methods proposed here no user-adjustments are necessary.

Runtime performance is catalogued in Table 1. The adaptive methods are observed to be about ten times faster than the comparable uniform-fine grid

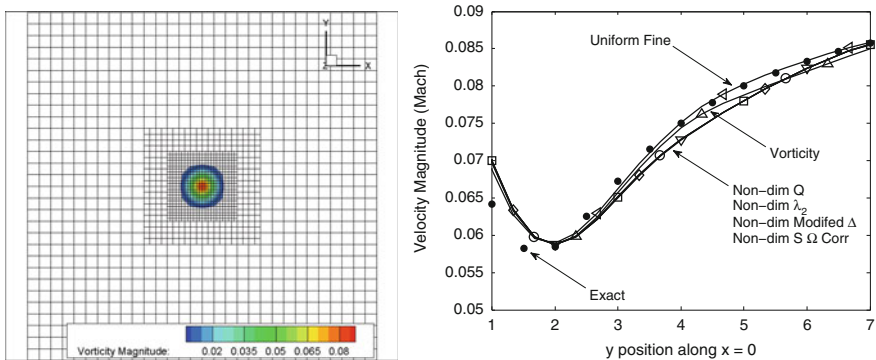


Fig. 1 Modified- Δ method applied to advecting vortex case (left). Comparison of methods after a single period (right)

Table 1 Comparison of average runtime per time-step and number of grid points for the single advecting vortex case on uniform and adaptive grids

	n	Sec/time-step
Coarse uniform	1.53×10^4	0.0742
Medium uniform	1.15×10^5	0.534
Fine uniform	8.93×10^5	4.19
Non-dim Q (adaptive)	1.04×10^5	0.305

computation. The coarse and medium uniform grid solutions, on the other hand, are observed to be highly dissipative in comparison.

3 Richardson Extrapolation-Based Error Estimation

The local truncation error (*LTE*) of the numerical scheme can be used as an indicator of the local error. *LTE* can be computed by using the difference between the exact and discrete solutions, i.e.,

$$\frac{u^{n+1} - w^{n+1}}{\Delta t} = \mathcal{O}(\Delta x^p) + \mathcal{O}(\Delta t^q) + \sum_{k=1}^{q-1} \mathcal{O}(\Delta x^p \Delta t^k). \tag{5}$$

This is verified in Fig. 2, where 5th-order accurate spatial discretization is observed for the advecting Lamb vortex case when it is run for several different values for Δt and Δx . Note that, for a given Δt , spatial refinement shows an initial fifth order error decrement, but eventually the temporal errors dominate and the error is observed to level off. Smaller Δt runs are observed to lead to a third-order accurate reduction in the temporal errors.

A major drawback of using the *LTE* to estimate the local error is that one typically needs an exact solution to develop an error estimate for the discrete solution. In practical cases where exact solutions do not exist, it is conceivable that the exact solution may be substituted by a discrete equivalent computed on a highly refined mesh. This concept describes the fundamental idea behind the Richardson extrapolation error estimation process.

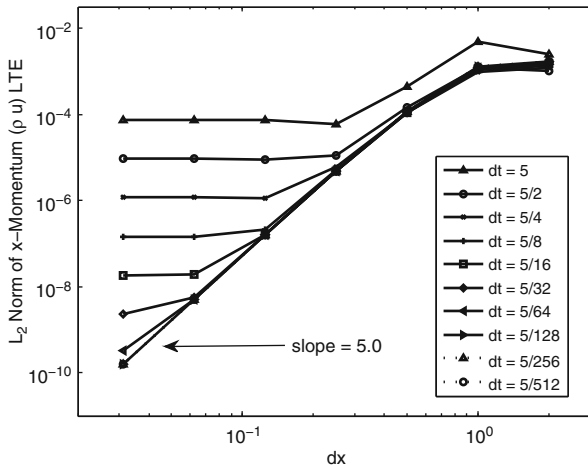


Fig. 2 *LTE* spatial convergence behavior of *x*-momentum (ρu) for the advecting vortex case

We can define the Richardson error estimation as follows:

$$E_{h/2} = \frac{w_{h/2} - w_h}{2^p - 1} + O(h^{p+1}). \tag{6}$$

Note that the denominator is a function of p , which is the order of accuracy employed by the finite difference scheme and is constant for the different grid levels. Indeed, the error expression is simply the difference between the solutions on the coarse and fine grids.

As in the case of the *LTE*, a similar accuracy analysis can be performed for the Richardson error estimator. It can be shown that, regardless of the number of refinement levels which exist between a coarse and fine solution, the error expression of Eq. (6) is

$$\frac{w_f^{n+1} - w_c^{n+1}}{\Delta t} \approx -\lambda \Delta x_c^p + \frac{\lambda^2 \Delta t}{2} \Delta x_c^p, \tag{7}$$

which indeed exhibits p th-order spatial accuracy. It is interesting to note the similarity to the unsteady *LTE* of Eq. (5). However, the Richardson error estimation contains only the spatial errors since the temporal errors are the same for the two grids and therefore cancel out. Thus, as the mesh is continually refined, the Richardson error estimator continues to converge at the rate corresponding to the spatial scheme. This behavior is illustrated by Fig. 3 where a coarse solution is compared against an extremely fine mesh. Furthermore, Fig. 3 also illustrates the case where the fine solution is calculated from the solution of the next level of refinement (rather than the highest level of refinement). This result also shows fifth order accuracy, demonstrating that the next level solution can be reliably used to define the local error. Additional testing of the above AMR approach for rotorcraft applications will be addressed in future work.

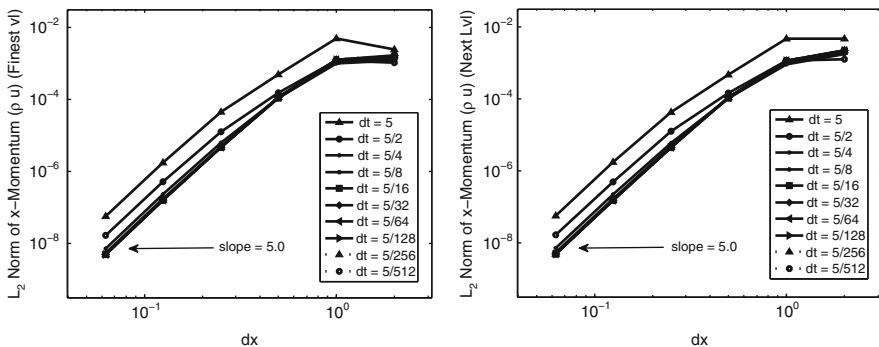


Fig. 3 Richardson spatial convergence behavior of x -momentum (ρu) for the advecting vortex case using a fine solution that has six levels of refinement. The plot on the *left* uses the finest level solution for calculating the error. The plot on the *right* uses the next level solution for calculating the error

4 Conclusion

This chapter has evaluated four distinct feature detection methods designed to drive Cartesian-based AMR in the off-body domain for vortex-dominated flows. Using traditional dimensional techniques to identify local regions for refinement, such as vorticity magnitude or the Q -criterion, can be problematic due to the requirement of a user-defined threshold which controls the refinement. Four particular non-dimensional schemes are evaluated: Q , λ_2 , Modified- Δ , and S - Ω correlation. It is shown that all the non-dimensional methods match the desirable performance without need for any parametric tuning. Additionally, the adaptive methods produce solutions that are comparable to the uniform-fine mesh equivalent, but are an order of magnitude faster. This chapter also lays the groundwork for using a Richardson Extrapolation error estimator to further control refinement for time-dependent flows. It is proposed that this error be utilized to provide a termination criterion to the AMR process. Future work will apply this feature-detection-based AMR methodology to a broader range of vortex-dominated flow-fields, particularly rotorcraft aeromechanics computations.

Acknowledgements Material presented in this chapter is a product of the CREATE-AV Element of the Computational Research and Engineering for Acquisition Tools and Environments (CRE-ATE) Program sponsored by the U.S. Department of Defense HPC Modernization Program Office. The article has been approved for public release by the AMRDEC Public Affairs Office (FN4345).

References

1. Aftosmis, M.J., Berger, M.J.: Multilevel error estimation and adaptive h-refinement for Cartesian Meshes with embedded boundaries. 40th AIAA Aerosciences Conference, Reno, AIAA Paper 2002-0863 (2002)
2. Chong, M.S., Perry, A.E., Cantwell, B.J.: A general classification of three-dimensional flow fields. *Phys. Fluids* **2**, 765–777 (1990)
3. Horiuti, K., Takagi, Y.: Identification method for Vortex sheet structures in turbulent flows. *Phys. Fluids* **17**(12), (2005)
4. Hunt, J.C.R., Wray, A.A., Moin, P.: Eddies, streams, and convergence zones in turbulent flows. In its Studying Turbulence using Numerical Simulation Databases, 2. Proceedings of the 1988 Summer Program, pp. 193–208, Stanford (SEE N89-24538 18-34) (1988)
5. Jeong, J., Hussain, F.: On the identification of a Vortex. *J. Fluid Mech.* **285**, 69–94 (1995)
6. Kamkar, S.J., Jameson, A.J., Wissink, A.M., Sankaran, V.: Feature-driven Cartesian adaptive mesh refinement in the Helios code. 48th AIAA Aerosciences Conference, Orlando, AIAA Paper 2010-0171 (2010)
7. Nemec, M., Aftosmis, M.J., Wintzer, M.: Adjoint-based adaptive mesh refinement for complex geometries. 46th AIAA Aerosciences Conference, Reno, AIAA Paper 2008-725 (2008)
8. Wissink, A.M., Sitaraman, J., Sankaran, V., Pulliam, T., Mavriplis, D.: A multi-code python-based infrastructure for overset CFD with adaptive Cartesian grids. 46th AIAA Aerosciences Conference, Reno, AIAA Paper 2008-927 (2008)